

Distributed quantum information processing with minimal local resources

Earl T. Campbell*

Department of Materials, Oxford University, Oxford, UK

(Dated: Feb, 2006)

We present a protocol for growing graph states, the resource for one-way quantum computing, when the available entanglement mechanism is highly imperfect. The distillation protocol is frugal in its use of ancilla qubits, requiring only a single ancilla qubit when the noise is dominated by one Pauli error, and two for a general noise model. The protocol works with such scarce local resources by never post-selecting on the measurement outcomes of purification rounds. We find that such a strategy causes fidelity to follow a biased random walk, and that a target fidelity is likely to be reached more rapidly than for a comparable post-selecting protocol. An analysis is presented of how imperfect local operations limit the attainable fidelity. For example, a single Pauli error rate of 20% can be distilled down to ~ 10 times the imperfection in local operations.

PACS numbers: 03.67.Mn, 03.67.Lx, 03.67.Pp

Entanglement distillation was first proposed to improve quantum communication channels by converting many noisy Bell pairs into fewer high-fidelity Bell pairs [1, 2, 3, 4]. Each half of a Bell pair is shared between distant locations, between which entanglement generation is noisy. Entanglement distillation is possible provided we can perform local operations and classical communication with significantly less noise than is present in the long-range channel. Following a swell of proposals for distributed quantum computing [5, 6, 7, 8, 9, 10, 11, 12, 13, 14], these protocols have found new applications in distilling entanglement between local sites of a distributed architecture [15, 16]. At each site there must be a certain number of qubits available, one logical qubit that is directly involved in the computation, and some number of ancilla qubits. In addition to distilling entanglement, using ancilla qubits protects the logical qubits against damage from probabilistic gates [10, 15, 16, 17]. The direct descendants of the quantum communication protocols create a high-fidelity Bell pair between two ancilla qubits, and then use this Bell pair to implement a two qubit gate between their logical qubits. Since these protocols emphasize implementing a good fidelity gate, we refer to them as *gate-based* protocols. For significant purification of noise from a general source, these proposals require 3 or 4 ancillary qubits [15, 16]; whereas for a restricted class of errors, the number of ancillary qubits can be reduced by one [16]. This paper proposes a protocol that requires one less ancilla for either noise source.

Another family of distillation protocols emerged after the one-way model of quantum computing showed that all the entanglement necessary for computation is present in a class of states called graph, or cluster, states [18, 19, 20, 21]. The distillation of graph states is akin to error correction, as the graph state is described by a group of stabilizers, and the purification process repeatedly measures the syndrome of these stabilizers. In virtue of this feature, we shall refer to this family of protocols as *stabilizer-based* protocols. The first such protocol used noisy copies of a graph state and post-selected upon detection of a single error [22, 23, 24]. However, the yield rapidly diminishes with the size of the graph state. Further proposals cast aside the need for post-selection at the cost of

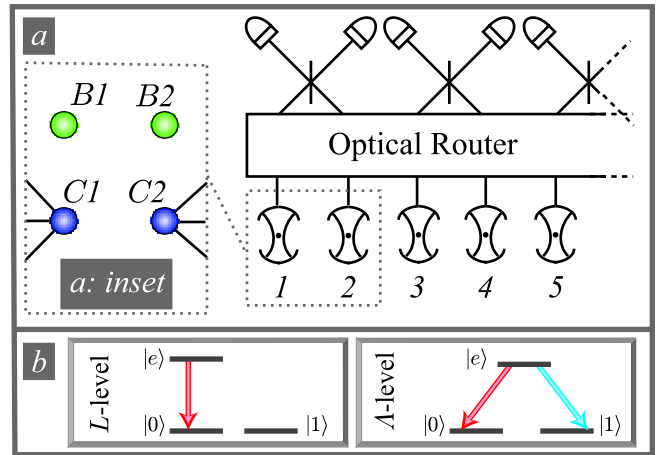


FIG. 1: An outline of a suitable architecture for a distributed quantum computer. (a) The numbers label local sites, each housing a matter system within an optical cavity. The optical cavities emit photons into an input port of a multiplexer, which can route any input port to any output port. Beam-splitters erase which-path information, so that entanglement is generated conditional on the detector signatures. (a: inset) for our primary protocol, each matter system is assumed to have enough level structure to provide two good qubits, a broker and a client. (b) two example level structures that would be suitable for the broker qubit. The L -level has only one logical state that optically couples to an excited state. The Λ -level structure has both levels coupling to a common excited state, however the two transitions are distinguishable by either frequency or polarization.

a stricter error threshold [25], above which, distillation is possible. These proposals use a combination of noisy copies of the graph state and highly purified GHZ states. Because of the size of the entangled states in the ancilla space, iterating these distillation protocols may take longer than for gate-based protocols. A significant temporal overhead will occur when the entangling operation has a high failure rate. Building large entangled states in the ancilla space also restricts the class of employable entangling operations, excluding entangling protocols that only produce Bell pairs [10, 11]. Of course, provided we have enough local qubits to provide ancillas for our ancillas, these disadvantages are easily nullified. However, it

is not yet clear that systems suitable for distributed quantum computation will have an abundance of suitable ancilla qubits.

In this paper we propose an entanglement distillation protocol that uses one less ancilla than previous protocols, and that inherits features from both families of entanglement distillation. The bulk of this paper will show that a single ancilla is sufficient to distil errors from a specific noise source. We then extend the protocol to cover general errors sources; as with other schemes this requires an additional ancilla, which we use to reduce the general noise to a specific noise. Like gate-based protocols, we build up a graph state edge-by-edge, with the ancillas never building entangled states larger than a Bell pair. However, as with stabilizer-based protocols, our proposal repeatedly makes stabilizer measurements directly onto the qubits constituting the graph state. As only a single ancilla is used for the bulk of the paper, we follow [17] and call the logical and ancillary qubit, the client and broker, respectively. The broker qubit must be optically active, such as in an L -level or Λ -level configuration (see Fig. 1b), and suitable for either entangling gates or operations that only generate Bell pairs. Furthermore, the optical transitions must respect a tensor product structure between the broker and client qubits; i.e. optical excitations of the broker must be possible without decohering the client. Suitable systems include two ions in an electromagnetic trap [10, 26], or an electron and nuclear spin of an NV-defect within diamond [17, 27, 28]. We outline the architecture of a distributed quantum computer in figure (1a), and introduce a qubit labelling that uses numbers for local sites and letters to distinguish broker and client qubits.

First our analysis will focus on the case when the noisy entanglement channel is dominated by one type of Pauli error, which may be very severe. Without loss of generality, we describe the channel as being affected by phase noise, such that two brokers $B1$ and $B2$, can be projected into the mixed state:

$$\rho_{B1,B2} = (1 - \varepsilon)|\Psi_+\rangle\langle\Psi_+| + \varepsilon Z_B|\Psi_+\rangle\langle\Psi_+|Z_B, \quad (1)$$

where Z_B is the Pauli phase-flip operator acting on either $B1$ or $B2$, and $|\Psi_+\rangle = |0\rangle_{B1}|1\rangle_{B2} + |1\rangle_{B1}|0\rangle_{B2}$. If the dominant noise is a different Pauli error, or different Bell pairs are produced, then local rotations can always bring the state into the form of equation 1. Furthermore, only a single Z error is possible as this bell state is invariant under the bilateral $Z_{B1}Z_{B2}$ rotation. Scenarios where such a noise model may arise include parity based entangling operations [5, 11] that possess a degree of robustness against bit-flip errors.

After producing noisy entanglement between two brokers, the entanglement is pumped down to the clients, resulting in a quantum operation on the client qubits. The target (perfect) entangling operation we aim to eventually achieve is either of the parity projections:

$$\begin{aligned} P_- &= 2(|01\rangle\langle 01| + |10\rangle\langle 10|), \\ P_+ &= 2(|00\rangle\langle 00| + |11\rangle\langle 11|), \end{aligned} \quad (2)$$

which act on the client qubits $C1$ and $C2$, and have an additional normalization factor of 2 that simplifies later expres-

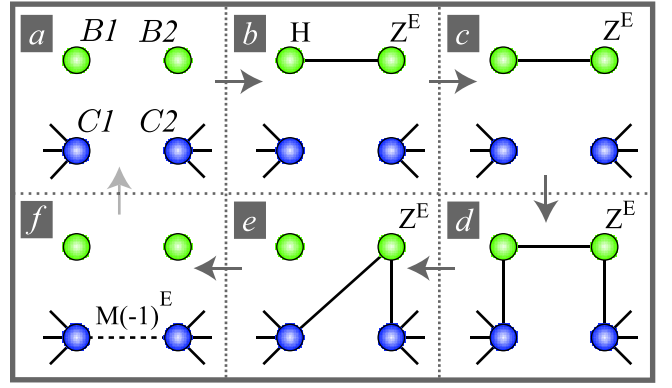


FIG. 2: The sequence of operations required to pump entanglement down to two client qubits $C1$ and $C2$, shown in the graph state notation. (a) Broker qubits are prepared in the $(|0\rangle + |1\rangle)/\sqrt{2}$ state, and the client qubits are part of some larger graph state $|\mathcal{G}\rangle$; (b) An entangling operation is performed between the broker qubits, with the possibility of Z noise; (c) A Hadamard is applied to one broker, $B1$; (d) At both local sites control- Z operations are performed between broker and client; (e) Broker $B1$ is measured in the Y basis; (f) Broker $B2$ is measured in the X -basis. The possibility of a Z error is tracked by using Z^E , where $E = 1$ tracks an error, and $E = 0$ tracks the errorless state. The measurement outcome is represented by M , where $M = +1$ for a $|0\rangle$ measurement and $M = -1$ otherwise. The dotted line between the client qubits represents a projection operator P_{\pm} between the client qubits, where the sign is equal to $M(-1)^E$.

sions. The only assumption we make about the initial state of the client qubits is that they are part of a graph state (in the constructive definition), such that they have equal magnitude in both parity subspaces, $\langle\mathcal{G}|P_+|\mathcal{G}\rangle = \langle\mathcal{G}|P_-|\mathcal{G}\rangle$; where $|\mathcal{G}\rangle$ denotes the graph state of all the client qubits. A successful P_- operation has the same effect on $|\mathcal{G}\rangle$ as type-II fusion [29], or a successful double heralding [5, 6], and can be used to build an arbitrary graph state; P_+ differs from P_- only by local rotations. We will see that entanglement distillation results from repetition of an entanglement transfer procedure.

Each round of our procedure is an entanglement pumping procedure, which we describe graphically in Fig. (2). Every round of purification begins with performing a noisy entangling operation between two broker qubits, $B1$ and $B2$. This operation may be probabilistic provided that success is *heralded*, in which case it is repeated until successful. Next, a series of local operations must be performed. First, apply a Hadamard to one broker, say $B1$, and then two control- Z operations between each broker and its client. The resulting state is a graph state, with the possibility of a Z error on $B2$, the broker qubit that did not undergo a Hadamard rotation. Then, measure $B1$ in the Y -basis and make any required rotations to correct for any by-product, and we now have the state described by Fig. 2e. Finally, $B2$ is measured in the X -basis. When no error was present, this measurement performs a parity check on the clients, $C1$ and $C2$; that is, we measure the observable $Z_{C1}Z_{C2}$. On the first round of pumping, the odd and even parity outcomes will occur with 50/50 probability. Accounting for the possibility of a Z error, the parity mea-

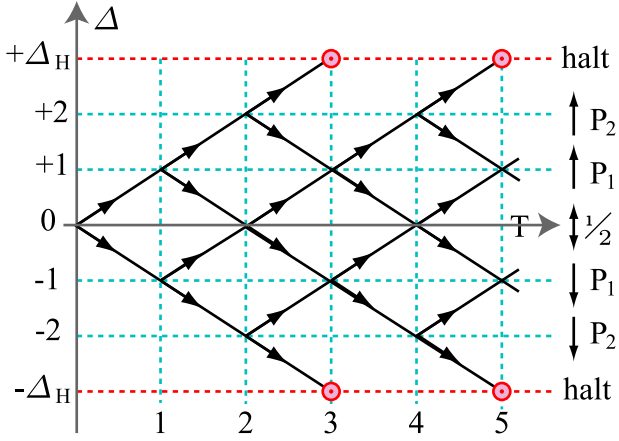


FIG. 3: The evolution of Δ against T , the number of rounds of entanglement pumping. The state evolves as a biased random walk in Δ . The weighting of probabilities at a some point Δ is such that there is a probability $P_{|\Delta|}$ for increasing the magnitude of Δ , where $P_{|\Delta|}$ is defined in equation 4. The red dashed lines represent the halting lines for Δ , and in this example $\Delta_H = 3$. Note that, the paths to the halting line, occur at $T = \Delta_H + 2n$, for non-negative integer n .

surement becomes noisy, such that the resulting projection is described by the quantum operation:

$$\mathcal{P}_{\Delta} (|\mathcal{G}\rangle\langle\mathcal{G}|) = \frac{\alpha^{\Delta} P_{+} |\mathcal{G}\rangle\langle\mathcal{G}| P_{+} + \alpha^{-\Delta} P_{-} |\mathcal{G}\rangle\langle\mathcal{G}| P_{-}}{\alpha^{\Delta} + \alpha^{-\Delta}}, \quad (3)$$

where $\alpha = (\varepsilon^{-1} - 1)^{\frac{1}{2}}$, and $\Delta = M1$ is +1 for a $|0\rangle$ measurement outcome, and -1 for $|1\rangle$.

If we repeat the entanglement pumping procedure n times, then we will get a series of measurements results $M1, M2, \dots, Mn$. Concatenating the quantum operation for each measurement result, we get back an operation of the same form but with $\Delta = \sum_{i=1}^n Mi$. The core of our proposal is that we continue to purify the client qubits until $|\Delta|$ reaches some value Δ_H at which point we halt the procedure. Δ_H is chosen such that it corresponds to a target fidelity F_T , where the fidelity is simply $F(\Delta) = (1 + \alpha^{-2|\Delta|})^{-1}$.

Compared to a standard gate-based protocol one difference is that the protocol is not post-selective (NPS). We can construct an analogous gate-based protocol that restarts upon any Mx that differs from $M1$, and hence is post-selecting (PS). Benefits of NPS are two-fold: (i) since purification is never restarted it is safe to operate directly on the client qubits, hence we eliminate the need for an additional broker qubit that exists in PS protocols; (ii) the probability of success within T rounds is never less than for PS, indeed, we shall show that NPS significantly outperforms PS in this regard. A point in favour of PS is that, if ancilla qubits are plentiful and local operations are imperfect, NPS may have a lower attainable fidelity. However, we shall see that does not prevent NPS from reaching fidelities within fault tolerance thresholds.

Returning to our consideration of the evolution of Δ in our protocol, it is clear that at each purification step, T , Δ can either increase or decrease by 1. Hence, the evolution bears

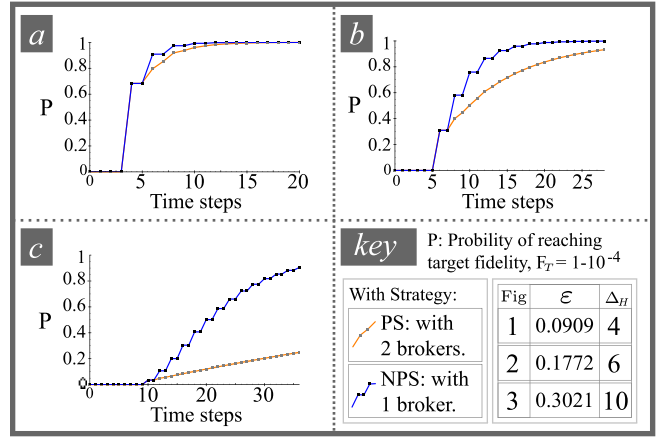


FIG. 4: A comparison of the rapidity of our proposal versus a post-selection protocol, with a target fidelity $F_T = 1 - 10^{-4}$. The three plots represent different values for the error rate ε , and hence require a different value of Δ_H ; shown in key. On each plot we show the probability of success against the number of rounds T , for both the protocol NPS (blue) and PS (orange). Notice that for NPS, the probability of success increases in steps. This is explained by figure 3, which shows that successful paths are separated by 2 time steps.

similarities to a random walk, illustrated by Fig.3. It differs from a random walk in two regards: (i) it halts when it reaches $\Delta = \pm|\Delta_H|$; (ii) the probabilities are the biased when $\Delta \neq 0$. The bias increases the chance of walking in the direction of larger $|\Delta|$, which occurs with probability:

$$P_D = \frac{(1 - \varepsilon)\alpha^D + \varepsilon\alpha^{-D}}{\alpha^D + \alpha^{-D}}, \quad (4)$$

where $D = |\Delta|$. On the face of it, it seems that the probability of walking to a state Δ in T steps is dependent upon which path is taken. However, the probability of a kink in the path — D increasing and subsequently decreasing — is independent of D , and is $k = P_D(1 - P_{D+1}) = \varepsilon(1 - \varepsilon)$. Hence, each path occurs with probability:

$$P_{\text{path}}(D, T) = \left(\prod_{d=0}^{D-1} P_d \right) k^{\left(\frac{T-D}{2}\right)}. \quad (5)$$

The total probability of walking to (D, T) is the product of $P_{\text{path}}(D, T)$ with the number of paths to that position.

We have calculated the total probability of success, after T rounds, by summing over all the different ways of reaching the halting line. For comparison, we performed the analogous calculation for an otherwise equivalent PS protocol. Figure 4 shows PS and NPS protocols for a target fidelity of $F_T = 1 - 10^{-4}$, with each plot being for a different error rate ε . Note that, for higher error rate or higher target fidelity, the width of the random walk is wider (larger Δ_H). In this regime, the superiority of NPS increases, as more entanglement can be lost upon post-selection. Conversely, when $\Delta_H = 2$ the protocols are effectively identical, as stepping back will take the walk to the origin.

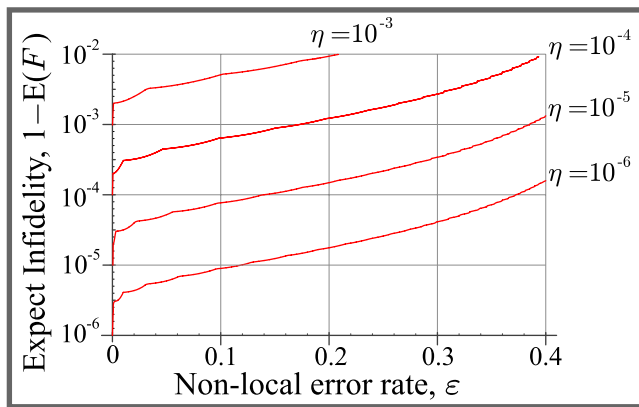


FIG. 5: A logarithmic plot of the expected infidelity, $1 - E(F)$, when additional error sources affect our distillation protocol. The plot is a function of ε , the probability of a specific Pauli error occurring in the long-range entangling operation, which is the error that the procedure is tailored to correct. Each curve is a different value of η , the probability per distillation round that some other error occurs.

For this idealized error model we can asymptotically approach unit fidelity. However, it is important to consider how other errors limit the maximum attainable fidelity. For simplicity, we take an aggressive error model where if a single error occurs once, then the overall entangling gate has fidelity zero. We use η to denote the probability per time step that an error occurs, where these errors can result from either faulty local operations or an error in the entanglement channel that is orthogonal to the dominant error that we are distilling. Furthermore, we approximate the chance of an error after T rounds by its upper bound, ηT . Once we reach Δ_H the fidelity will depend on the number of time steps taken. Therefore, we calculate the expectation of the fidelity, $E(F)$. Figure 5 shows how the expected infidelity, $1 - E(F)$, varies with ε , for different values of η . Since the optimal choice of Δ_H changes with ε this produces inverted humps along the curves, which are more pronounced for small ε . On all curves the behaviour is roughly the same; we can characterize the performance by noting that when the dominant error rate is 0.2 (i.e. 20%), and the probability of other error sources is η , then the protocol brings *all* error probabilities to order 10η .

If the orthogonal errors are significant, then an additional ancilla is employed. Using these two ancillas bit-errors are distilled away, by a post-selecting protocol such as in [16]. The most symmetric noise has each Pauli error occurring with equal probability, producing Werner states of fidelity F_0 . Distilling bit-errors to order η takes $n = \ln(\eta)/\ln(2\xi)$ rounds of distillation; where $3\xi = 1 - F_0$. The resulting noisy Bell-pair is dominated by phase-noise, of amount $\varepsilon = \sum_{i:\text{odd}}^n B(n, i)\xi^i(1 - \xi)^{n-i}$; where $B(n, i)$ is the binomial. For example, distilling Werner states of Fidelity $F_0 = 0.85$, the bit-errors can be reduced to 10^{-5} , and the phase error rate becomes $\varepsilon = 0.205$. These Bell pairs, with their asymmetric errors, are used in our primary distillation protocol.

In conclusion, using fewer ancilla qubits than in previous proposals, an otherwise intolerably-large error is rapidly re-

duced to within error-correction thresholds [30, 31]. For an asymmetric and a symmetric noise model, the protocols needs only one and two ancilla qubits, respectively. Note that, an entangling operation suitable for construction of GHZ states in the broker space permits a marriage of the weighted walk strategy and the band-aid protocol [25]. Such an approach to distillation would be more robust against imperfect local operations. The author thanks Simon Benjamin, Joseph Fitzsimons, Pieter Kok, and Dan Browne for useful discussions. This research is part of the QIP IRC (GR/S82176/01).

* Electronic address: earl.campbell@materials.ox.ac.uk

- [1] C. H. Bennett et al., Phys. Rev. Lett **76** (1996).
- [2] C. H. Bennett et al., Phys. Rev. A **54** (1996).
- [3] W. Dür et al., Phys. Rev. A **59**, 169 (1999).
- [4] M. Murao et al., Phys. Rev. A **57**, R4075 (1998).
- [5] S. D. Barrett and P. Kok, Phys. Rev. A **71**, 060310 (2005).
- [6] S. C. Benjamin, Phys. Rev. A **72**, 056302 (2005).
- [7] S. C. Benjamin, J. Eisert, and T. M. Stace, New J. Phys. **7**, 194 (2005).
- [8] S. Bose et al., Phys. Rev. Lett **83**, 5158 (1999).
- [9] C. Cabillo et al., Phys. Rev. A **59**, 1025 (1999).
- [10] L. M. Duan et al., Quantum Information and Computation **4**, 165 (2004).
- [11] L. M. Duan and H. J. Kimble, Physical Review Letters **90**, 253601 (2003).
- [12] X. L. Feng et al., Phys. Rev. Lett **90**, 217902 (2003).
- [13] Y. L. Lim et al., Phys. Rev. A **73**, 012304 (2006).
- [14] Y. L. Lim, A. Beige, and L. C. Kwak, Phys. Rev. Lett **95**, 030505 (2005).
- [15] W. Dür and H. J. Briegel, Phys. Rev. Lett. **90**, 067901 (2003).
- [16] L. Jiang et al., (2007), quant-ph/0703029.
- [17] S. C. Benjamin et al., New Journal of Physics **8**, 141 (2006).
- [18] M. Hein et al., (2005), quant-ph/0602096.
- [19] M. Hein, J. Eisert, and H. J. Briegel, Phys. Rev. A **69**, 062311 (2004).
- [20] R. Raussendorf and H. J. Briegel, Phys. Rev. Lett. **86**, 5188 (2001).
- [21] R. Raussendorf, D. E. Browne, and H. J. Briegel, Phys. Rev. A **68**, 022312 (2003).
- [22] H. Aschauer, W. Dür, and H. J. Briegel, Physical Review A **71**, 012319 (2005).
- [23] W. Dür, H. Aschauer, and H. J. Briegel, Phys. Rev. Lett. **91**, 107903 (2003).
- [24] C. Kruszynska et al., Physical Review A **74**, 052316 (2006).
- [25] K. Goyal, A. McCauley, and R. Raussendorf, Physical Review A **74**, 032318 (2006).
- [26] D. K. L. Oi, S. J. Devitt, and L. C. L. Hollenberg, Physical Review A **74**, 052313 (2006).
- [27] T. Gaebel et al., , Nature Physics **2**, 408 (2006).
- [28] J. Wrachtrup, S. Y. Kilin, and A. P. Nizovtsev, Optics and Spectroscopy **91**, 429 (2001).
- [29] D. E. Browne and T. Rudolph, Phys. Rev. Lett **95**, 010501 (2005).
- [30] R. Raussendorf, J. Harrington, and K. Goyal (2007), quant-ph/0703143.
- [31] C. M. Dawson, H. L. Haselgrove, and M. A. Nielsen, Physical Review Letters **96**, 020501 (2006).